N-36-CR
210982
398

PROGRESS REPORT

SUBMITTED TO :	*National Aeronautics and Space Administration Langley Research Center Hampton, Virginia 23665*
INSTITUTION:	*Department of Physics Hampton University Hampton, Virginia 23668*
TITLE OF RESEARCH:	*Development of Mid-Infrared Solid State Lasers for Spaceborne Lidar*
NASA GRANT NUMBER:	*NAG-1-877* ✓
PERIOD COVERED BY THIS REPORT:	*October 13, 1988 - April 13, 1989*
PRINCIPAL INVESTIGATOR:	*Donald A. Whitney*
CO-PRINCIPAL INVESTIGATOR:	*Kyong H. Kim*

(NASA-CR-185012) DEVELOPMENT OF MID-INFRARED SOLID STATE LASERS FOR SPACEBORNE LIDAR Progress Report, 13 Oct. 1988 - 13 Apr. 1989 (Hampton Inst.) 39 p CSCL 20E G3/36

N89-24599

Unclas 0210982

CONTENTS

SUMMARY

This semiannual progress report covers work performed during the period from October 13, 1988 to April 13, 1989 under NASA grant number NAG-1-877 entitled "Development of mid-infrared solid state lasers for spaceborne lidar". During this period we have measured the laser performance of a Ho^{3+}:Tm^{3+}:Cr^{3+}:YAG crystal under flashlamp pumping at various operating temperatures. The normal-mode laser thresholds of a Ho^{3+}(0.45 at. %):Tm^{3+}(2.5 at. %):Cr^{3+}(1.5 at. %):YAG crystal were found to range from 26 to 50 J between 120 and 200 Kelvin with slope efficiencies up to 0.36 % with a 60 % reflective output mirror. From the Q-switched operations a slope efficiency corresponding to 90 % of the normal-mode operation was observed. Laser wavelengths were measured for various operating conditions and fluorescence spectra were obtained at various temperatures in order to help understand the dynamic energy processes among the Ho^{3+}, Tm^{3+} and Cr^{3+} ions. A pulse forming network for a flashlamp pumped Cr:GSAG laser, which is to be used as a high power laser diode simulator in rare earth laser pumping, was completed and tested. The network provided critically damped, 1 ms FWHM, square pulses with a rise time of about 160 μs at an input electrical energy of 300 J.

INTRODUCTION

A flashlamp-pumped laser system cooled with nitrogen-vapor and modified for 60 J electrical input energy and 350 μs pulse width (FWHM) during the previous six-month period has been employed for laser performance measurements of a Ho^{3+}:Tm^{3+}:Cr^{3+}:YAG crystal. The main concern of this research was focused on determination of optimum Tm^{3+} concentration in Ho^{3+}:Tm^{3+}:Cr^{3+}:YAG crystals for efficient Q-switched laser output by studying laser performance of the Ho^{3+}:Tm^{3+}:Cr^{3-}:YAG crystals with different Tm^{3+} concentrations at relatively fixed Ho^{3+} and Cr^{3+} concentrations. Coherent Laser Technology provided three Ho^{3+}:Tm^{3+}:Cr^{3+}:YAG crystals with Tm^{3+} concentrations of 2.5, 3.5 and 4.5 at. %, respectively, and with the same 0.45 at. % Ho^{3+} and 1.5 at. % Cr^{3+} concentrations. During this research period normal-mode and Q-switched laser performance and fluorescence spectroscopy of the Ho^{3+} (0.45 at. %): Tm^{3+} (2.5 at. %):Cr^{3+} (1.5 at. %):YAG crystal were studied under various operating conditions. Laser output energy, slope efficiency, energy threshold, Q-switched pulse length and laser wavelength were determined as a function of operating temperature, output mirror reflectivity, input electrical energy and Q-switch opening time. Fluorescence measurements were also performed at various wavelengths and temperatures to understand the lifetime of excited levels and possibly to obtain information about energy transfer processes among the multiple ions.

We have also completed and tested a pulse forming network of input energy 300 J and pulse widths longer than 1 ms FWHM for a flashlamp-pumped Cr^{3+}:GSAG laser. This network will be used to simulate a high power laser diode in pumping mid-infrared rare earth laser crystals such as Tm^{3+}, Er^{3+} and/or Ho^{3+}-ion doped YAG, YLF or other host materials. This Cr^{3+}:GSAG laser will be used to determine optimum conditions for laser diode pumped mid-infrared lasers, maximum energy extraction limit with longitudinal pumping, thermal damage limit, and other problems related to high power laser diode pumping.

One full-time graduate student and two undergraduate students were involved in this project to perform and to assist the research activity.

RESULTS OF THE FLASHLAMP-PUMPED $Ho^{3+}:Tm^{3+}:Cr^{3+}:YAG$ LASER EXPERIMENT

Part of the Normal-mode and Q-switched laser results obtained from the flashlamp-pumped $Ho^{3+}:Tm^{3+}:Cr^{3+}:YAG$ laser experiment was presented at the NASA HBCU Forum held March 22-23, 1989 at Huntsville, Alabama and is attached in the Appendix.

Fig.1 shows the experimental setup used to measure the laser intensity at various wavelengths for the $Ho^{3+}:Tm^{3+}:Cr^{3+}:YAG$ laser. These measurements are shown in Figs.2 through 5. Fig.2 shows that laser wavelengths are observed at 2.098 and 2.091 μm during normal-mode operation with a Ho^{3+}(0.45 at. %):Tm^{3+}(2.5 at. %):Cr^{3+}(1.5 at. %):YAG crystal, a 60 J input electrical energy and a 60 % reflective output mirror at various operating temperatures. The 2.098 μm line was assigned to the transition from the lowest manifold of the upper $^5I_7$ state at ≈5230 cm^{-1} to the manifold of the ground $^5I_8$ state at 462 cm^{-1}. [Refs.1 and 2] No significant change of the laser wavelengths was observed as the operating temperature was changed from 130 K to 170 K and the input energy was changed from 45 J to 60 J as shown in Figs.2 and 3.

Fig.4 shows the comparison of laser wavelengths observed in a normal-mode operation with that in a Q-switched operation. An output mirror of 60 % reflectivity, input electrical energy of 45 J and operating temperature of 150 K were used for this measurement. The $LiNbO_3$ Q-switch crystal and a ZnSe plate set at Brewster's angle were also in place during the normal-mode operation. No significant change of the laser wavelengths was observed during either operating mode. Fig.5 shows that the 2.091 μm laser line disappeared when the output mirror reflectivity was changed from 60 % to 98 %.

Fluorescence of the Ho^{3+}:Tm^{3+}:Cr^{3+}:YAG crystal was measured at various temperatures and input energies with the setup drawn in Fig.6. Figs.7 through 10 show the change of the 2.1 μm fluorescence risetime, decay time, peak intensity and peak position as a function of temperature. The risetime and decay time were taken by reading the time between the 10 % and 90 % peak value points. The change of the risetime of the 2.1 μm fluorescence with temperature includes the thermal dependence of upper state lifetime and the energy transfer rate from Cr^{3+} to Tm^{3+} ions and from Tm^{3+} to Ho^{3+} ions as well as the thermal population of the upper ground state manifolds.

The measured 1.9 and 1.7 μm fluorescence patterns of the Ho^{3+}:Tm^{3+}:Cr^{3+}:YAG crystal are shown in Figs.11 through 16. As the operating temperature increases, the 2.1 μm fluorescence peak intensity decreases and the 1.9 μm and 1.7 μm fluorescence peak intensities increase. This agrees with the spectral measurement of a Ho^{3+}:Tm^{3+}:YAG crystal done by Armagan [Ref.3]. The 2.1 μm fluorescence peak originating from the Ho^{3+}-ions gradually shifts to 1.9 μm and combines with the 1.9 μm fluorescence of the Tm^{3+} ions. As the temperature increases, the 1.9 μm fluorescence originating from the Tm^{3+} ions becomes weak and shifts to 1.7 μm. It was shown that the 1.7 μm fluorescence did not appear at low temperatures but became stronger as the temperature increased. A theoretical modeling to explain these phenomena and to relate them with laser performance is under investigation at the present time.

PULSE-FORMING-NETWORK FOR FLASHLAMP PUMPED Cr:GSAG LASER

During this report period we have completed and tested a pulse-forming-network for a flashlamp pumped Cr:GSAG laser system which is to used to simulate a high power laser diode in pumping rare earth ion (such as Tm^{3+} and Ho^{3+}) doped crystals and to study various problems involved with high power laser diode pumping. Since the lifetime of the upper laser level is relatively long, approximately 8 ms at room temperature, a long pump pulse is expected to achieve a high efficiency. Based on the design parameters calculated during the previous research period, a pulse-forming-network of input energy 300 J and pulse width of longer than 1 ms FWHM was completed. The typical flashlamp pulse signal was analyzed and the results are shown in Figs.17 through 19. Fig.17 shows the total optical signal observed from a 3" arc length and 4 mm bore diameter flashlamp at electrical input energy 300 J in a 3 LC section pulse forming network with sectional capacitance and inductance of 150 μF and 185 μH, respectively.

Figs. 18 and 19 show the flashlamp light observed at 296 nm and 450 nm, respectively, for an electrical input energy of 300 J. Fig.20 shows the increase of the flashlamp light at 450 nm as a function of electrical input energy measured within a linear region of the detector.

Fig.21 shows the amount of cut-off of UV light by a uranium doped quartz flow tube compared to a pure quartz glass tube. Since the uranium doped flow tube transmits 450 nm light, the cut-off of 296 nm light compared to the 450 nm light was found for the two kinds of flow tubes. Improved cut-off of UV light was observed as shown in Fig.21. UV light is known to be detrimental for the Cr:GSAG laser because of possible color center effects and other UV induced optical losses.

CONCLUSION

We have measured 2.1 μm laser performance of a Ho^{3+}(0.45 at. %):Tm^{3+}(2.5 at. %):Cr^{3+}(1.5 at. %):YAG crystal under flashlamp pumping at various operating temperatures. Both normal-mode and Q-switched performance were investigated. Laser wavelength and fluorescence measurement were also performed for the crystals. During the following research period similar measurements will be performed for two more crystals with different Tm^{3+} concentrations provided by Coherent Laser Technology to determine an optimum Tm^{3+} concentration in the Ho:Tm:Cr:YAG crystal. In addition, a theoretical modeling to explain the observed data will be made.

During the past six-month research period a pulse-forming-network for Cr:GSAG laser has been completed and tested. A nearly square shape pulse with pulse length of ≈1 ms was observed with a 3" arc length and 4 mm bore diameter flashlamp at an electrical input energy of 300 J. An UV filtering effect by an uranium doped flow tube was also measured. During the next research period further filtering of UV light will be performed, and a flashlamp pumped Cr:GSAG laser system will be completed and tested for rare earth laser pumping.

REFERENCES

1. L. F. Johnson, J. E. Geusic, and L. G. Van Uitert, "Coherent oscillations from Tm^{3+}, Ho^{3+}, Yb^{3+}, and Er^{3+} ions in yttrium aluminum garnet," Appl. Phys. Lett., **7**, 127 (1965).
2. T. Y. Fan, G. Huber, R. L. Byer, and P. Mitzscherlich, "Spectroscopy and Diode Laser-Pumped Operation of Tm, Ho:YAG," IEEE J. Quantum Electron. **24**(6), 924 (1988).
3. G. Armagan (Christopher Newport College/ NASA Langley Research Center), private communications, (1989).

List of Figures

various input energies.

Figure 12. 1.9 μm fluorescence decay time of a 0.45Ho:2.5Tm:1.5Cr:YAG crystal as a function of operating temperature at various input energies. (Decay time was taken from 10% and 90% of the peak intensity.)

Figure 13. 1.9 μm fluorescence peak intensity of a 0.45Ho:2.5Tm:1.5Cr:YAG crystal as a function of temperature at various input energies.

Figure 14. 1.9 μm fluorescence peak position of a 0.45Ho:2.5Tm:1.5Cr:YAG crystal with respect to the beginning of the fluorescence pulses as a function of operating temperature at various input energies.

Figure 15. 1.7 μm fluorescence risetime and peak intensity of a 0.45Ho:2.5Tm:1.5Cr:YAG crystal as a function of temperature. (Input electrical energy = 60 J)

Figure 16. 1.7 μm fluorescence peak position and risetime of a 0.45Ho:2.5Tm:1.5Cr:YAG crystal as a function of temperature at an input electrical energy of 60 J.

Figure 17. Total optical flashlamp light measured with a silicon photodiode. A 300 J input energy was used in a 3 LC section PFN designed to have critically damping for that energy and 1 ms pulse width with sectional capacitance and inductance of 150 μF and 185 μH, respectively.

Figure 18. Flashlamp light signal taken with a 296.3 nm narrow band filter at a input energy of 300 J.

Figure 19. Flashlamp light signal taken with a 450 nm narrow band filter at a input energy of 300 J.

Figure 20. Flashlamp light at 450 nm as a function of electrical input energy.

Figure 21. Ratio of flashlamp light intensity at 296 nm to that at 450 nm is shown as a function of electrical input energy to compare a uranium doped flow tube to a quartz flow tube for UV cut-off effect.

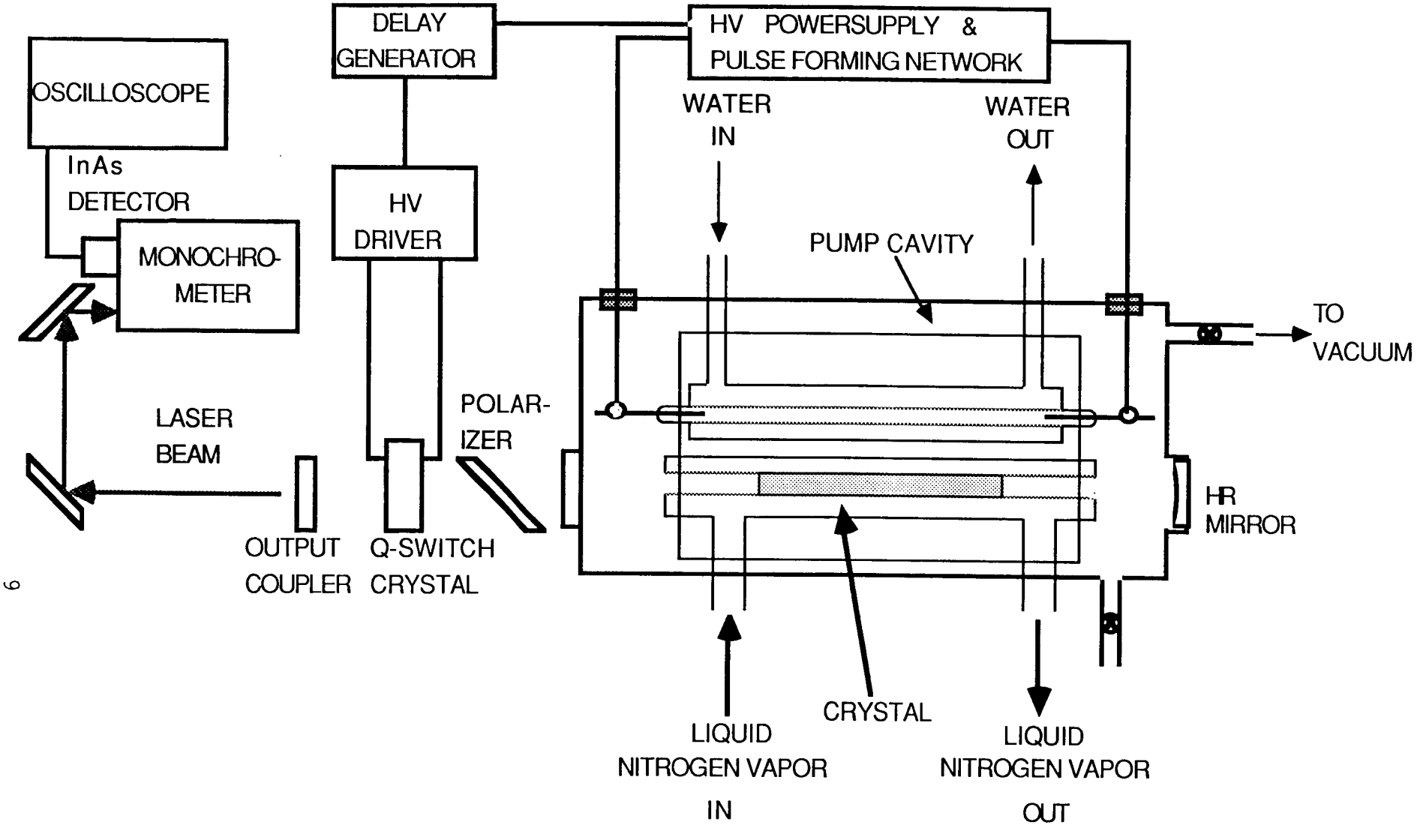

Fig.1 Experimental setup for laser wavelength measurement.

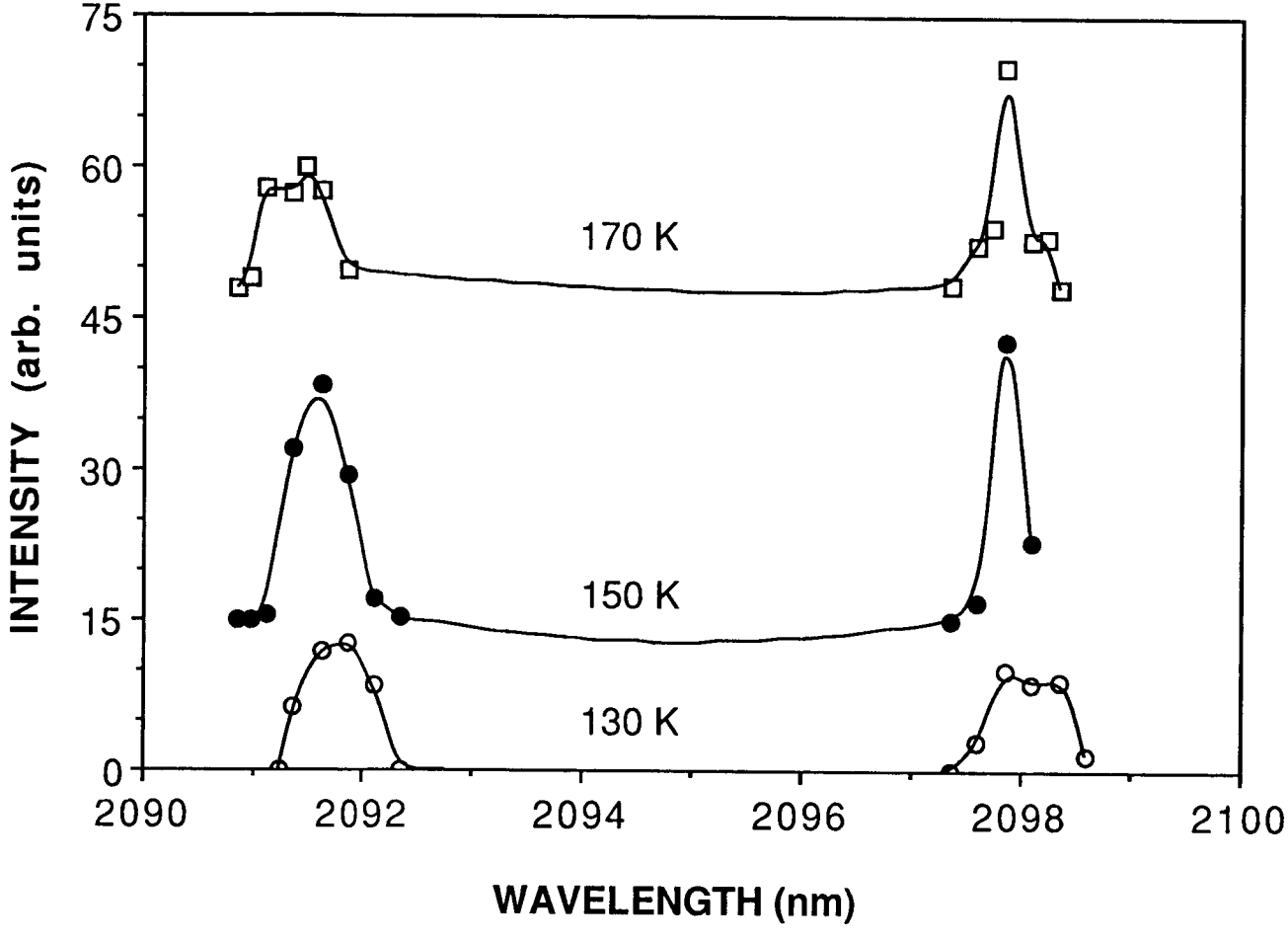

Fig.2 Laser wavelengths of a 0.45Ho:2.5Tm:1.5Cr:YAG laser observed during normal-mode operations with a 60% reflective output mirror and an input electrical energy of 60 J.

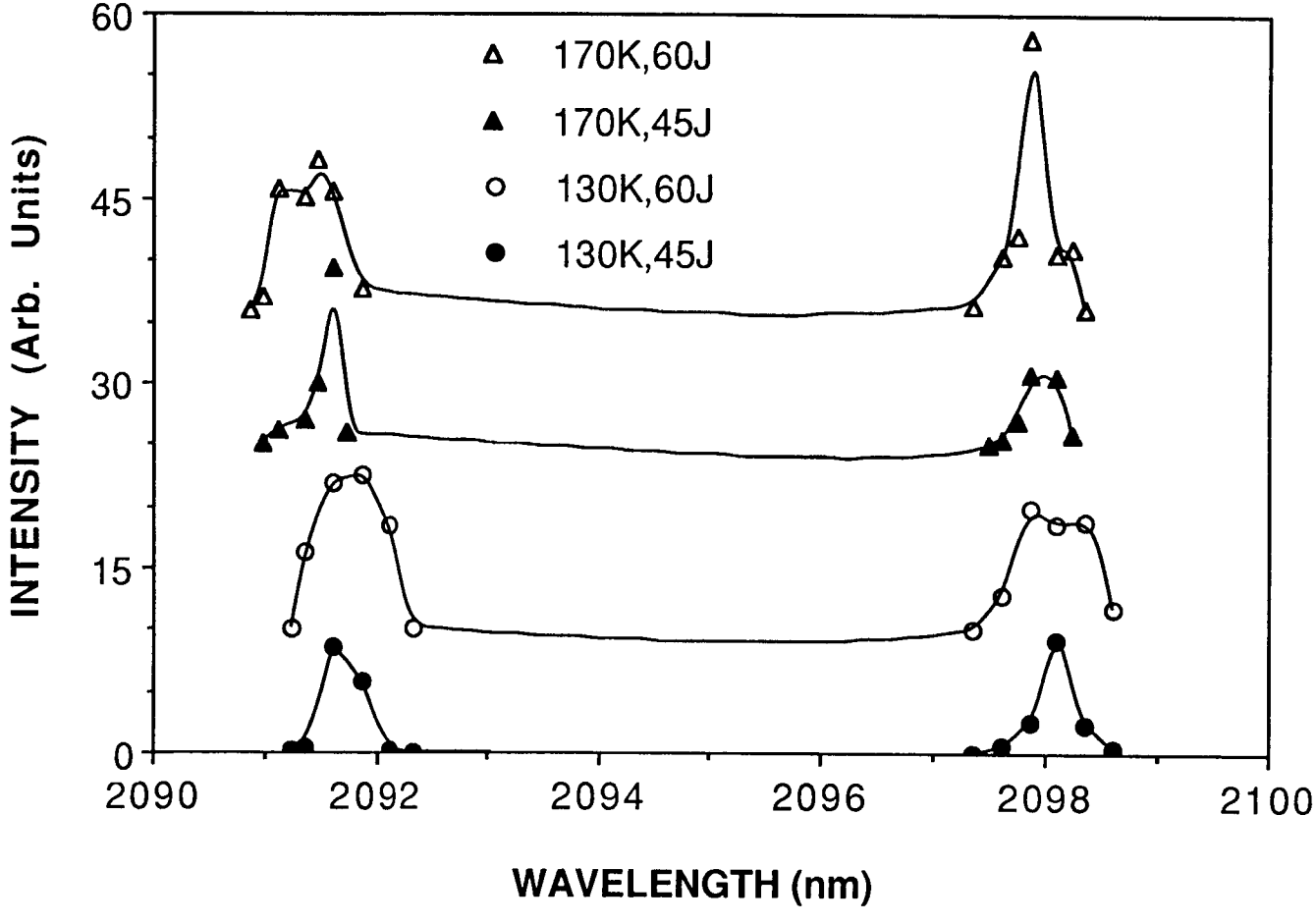

Fig.3 Laser wavelengths of a 0.45Ho:2.5Tm:1.5Cr:YAG laser observed during normal-mode operations at various operating temperatures and input energies with a 60% reflective output mirror.

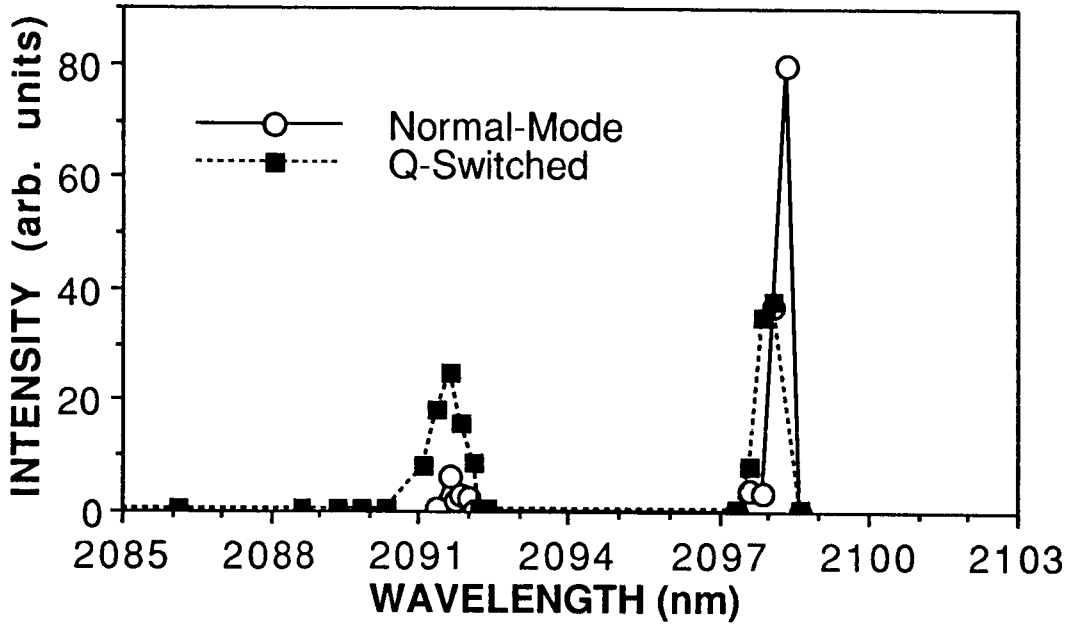

Fig.4 Observed laser wavelengths during normal-mode and Q-switched operations at operating temperature of 150K, input electrical energy of 45J and output mirror reflectivity of 60%. (Q-switch was in resonator during normal-mode.)

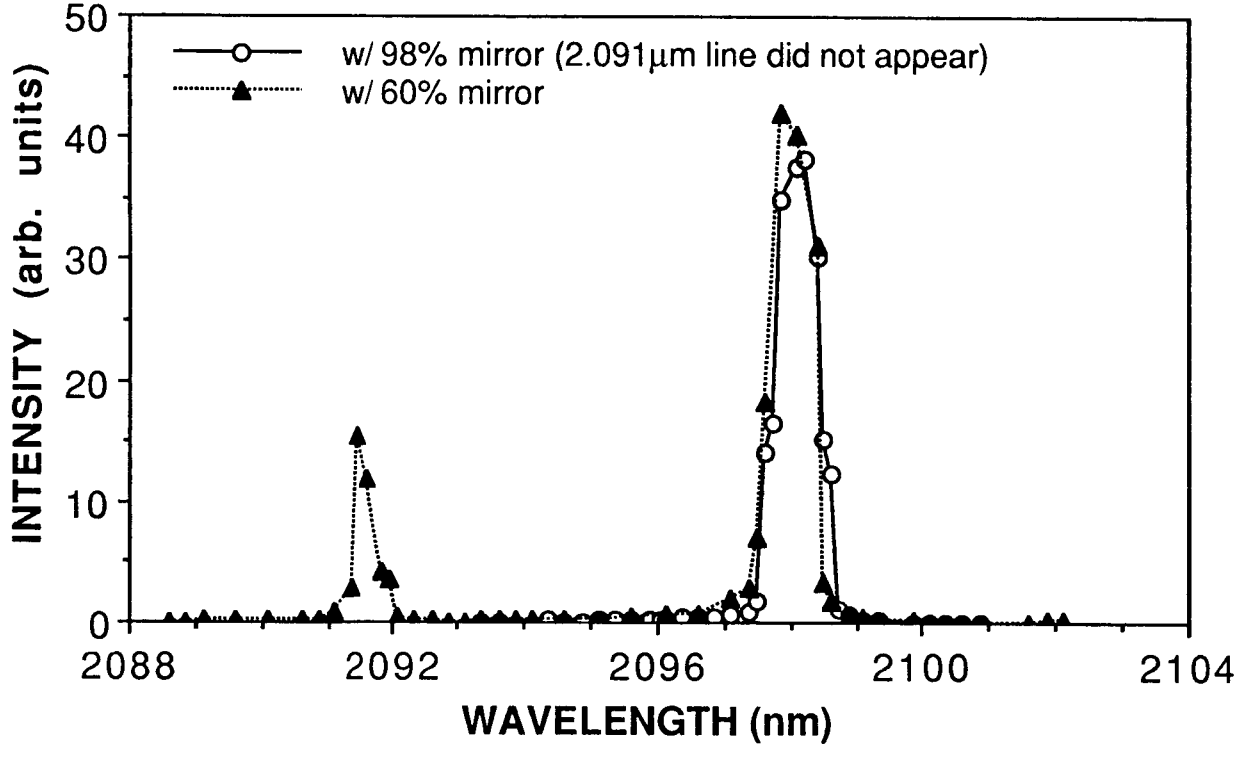

Fig.5 Laser wavelengths observed with 60% and 98% reflective output mirrors, respectively, during normal-mode operation at T=150K and Ein=60J.

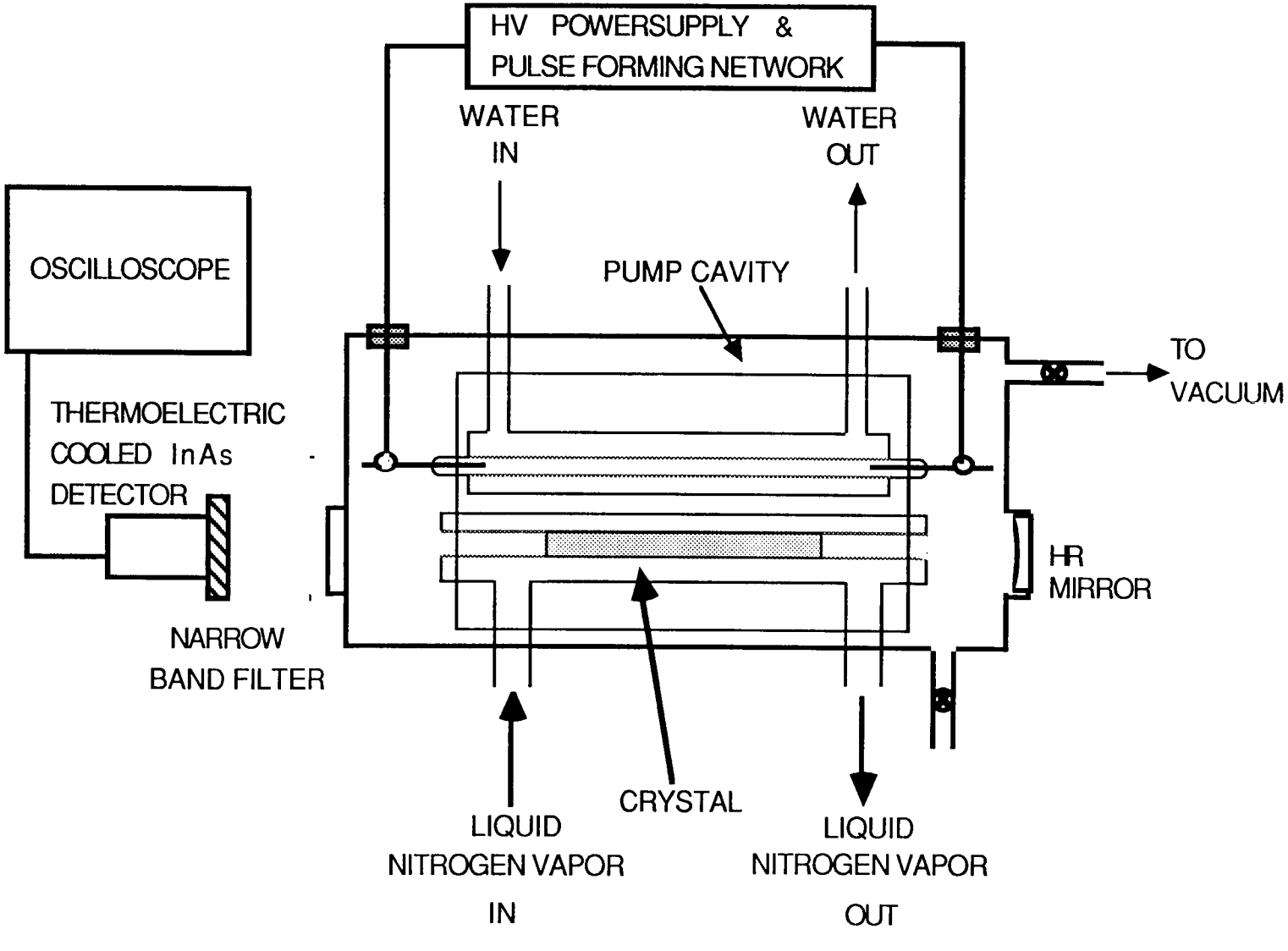

Fig.6 Experimental setup for fluorescence measurement

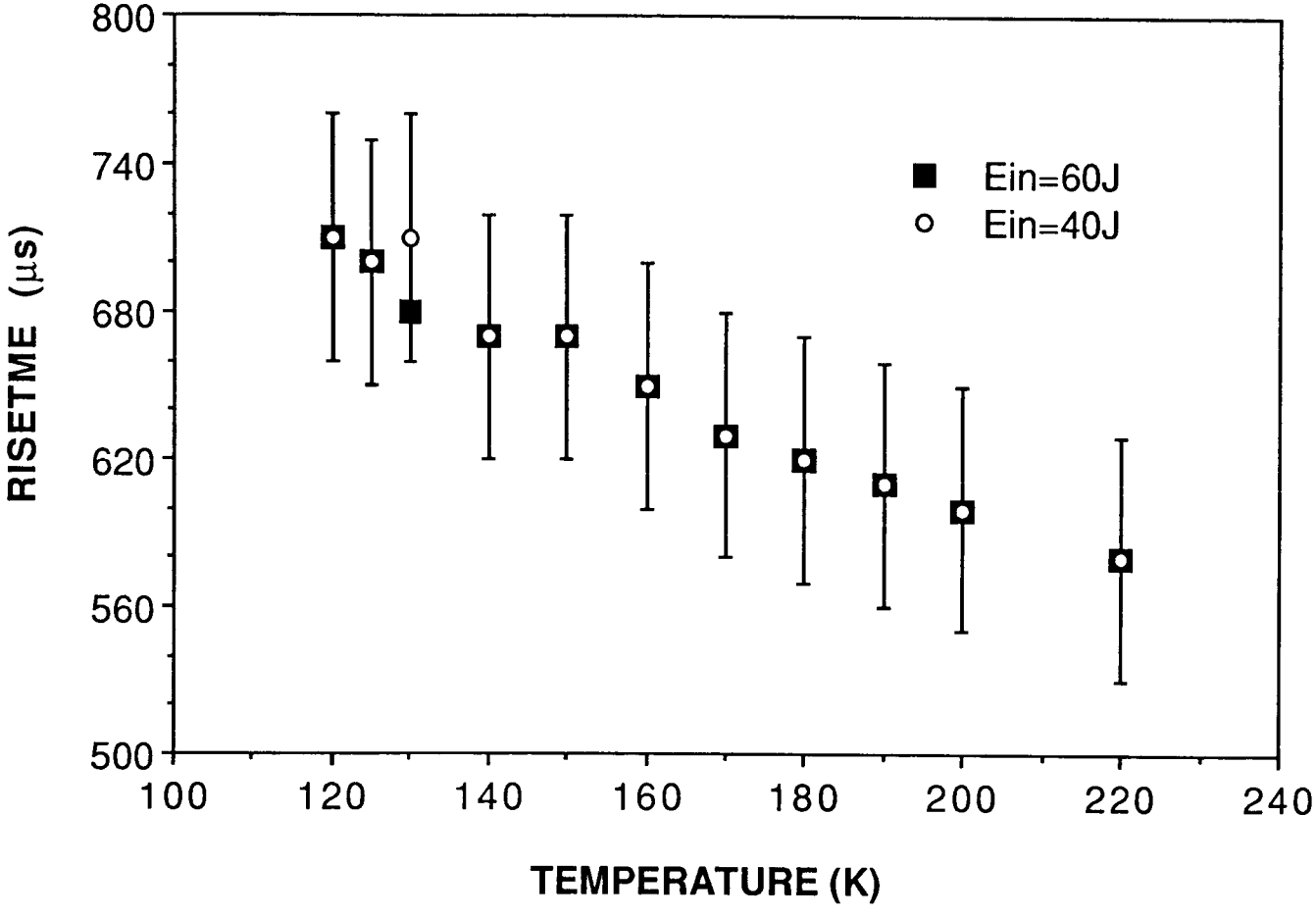

Fig.7 2.1μm fluorescence risetime of a 0.45%Ho:2.5%Tm:1.5%Cr:YAG crystal observed at various operating temperatures and electrical input energies.

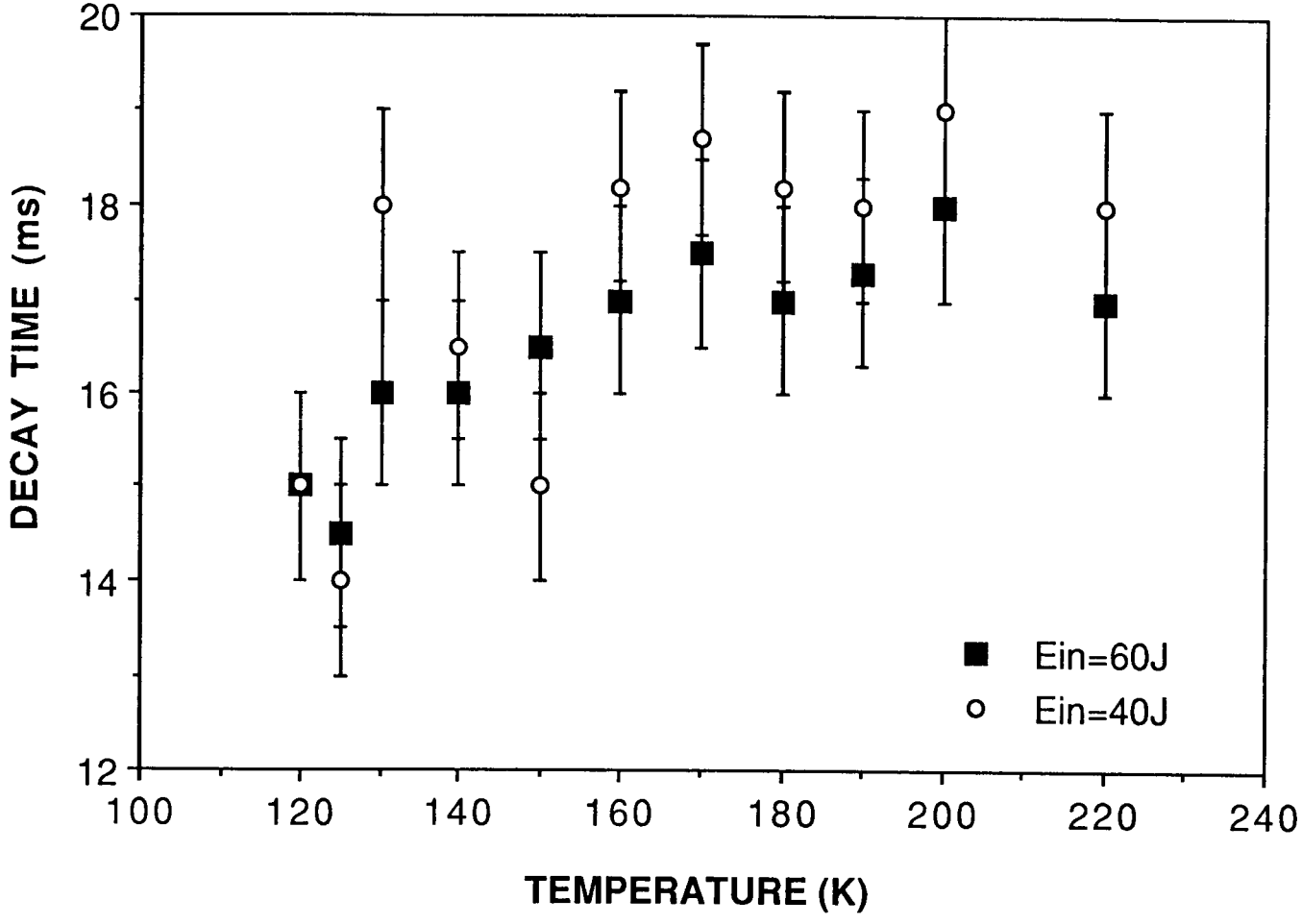

Fig.8 2.1μm fluorescence decaytime of a 0.45Ho:2.5Tm:1.5Cr:YAG crystal as a function of temperature. (Decay time was taken from 10% and 90% of the peak intenisty.)

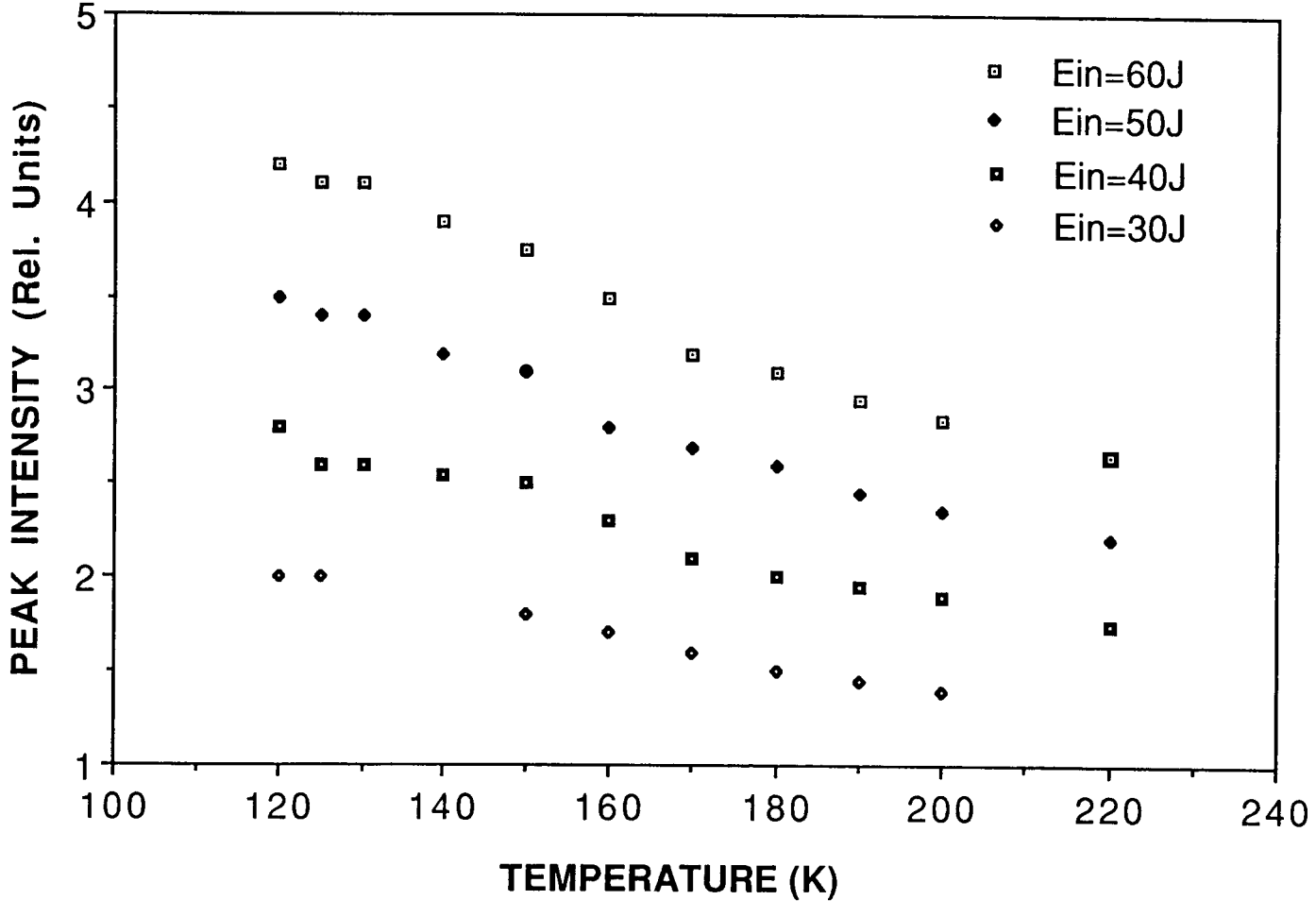

Fig.9 2.1μm fluorescence peak intensities observed from a 0.45Ho:2.5Tm:1.5Cr:YAG crystal as a function of operating temperature at various input energies.

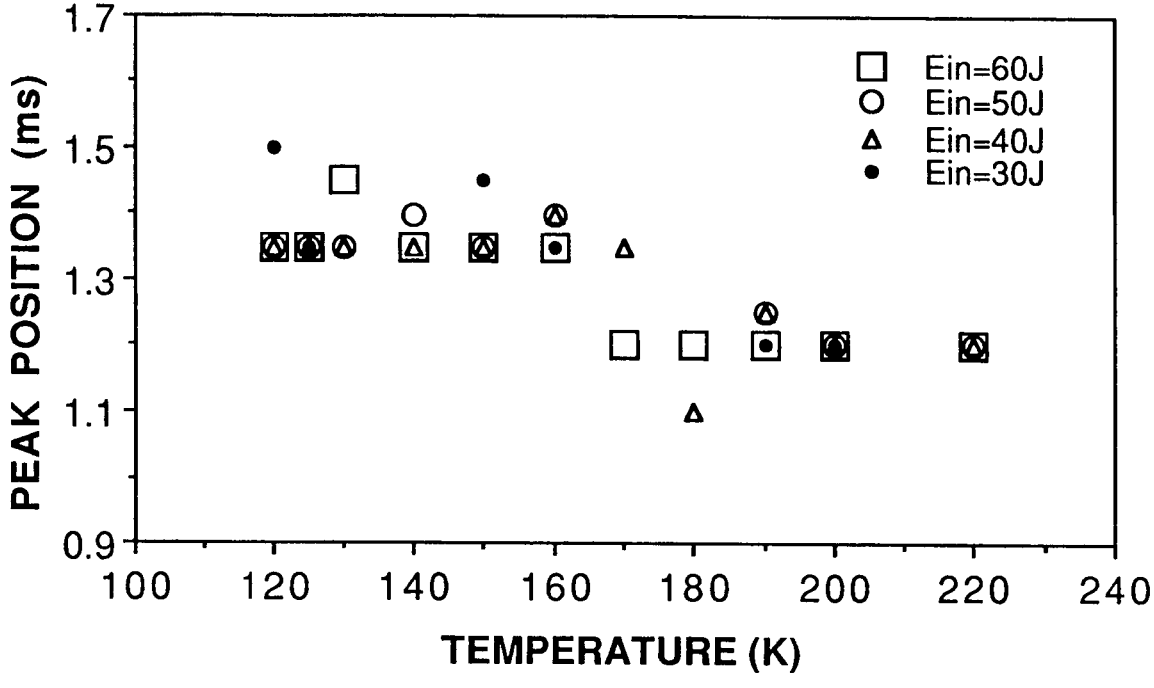

Fig. 10. 2.1 μm fluorescence peak appearance time of a 0.45 Ho:2.5 Tm: 1.5 Cr:YAG crystal with respect to the beginning of the fluorescence pulses as a function of operating temperature at various input energies.

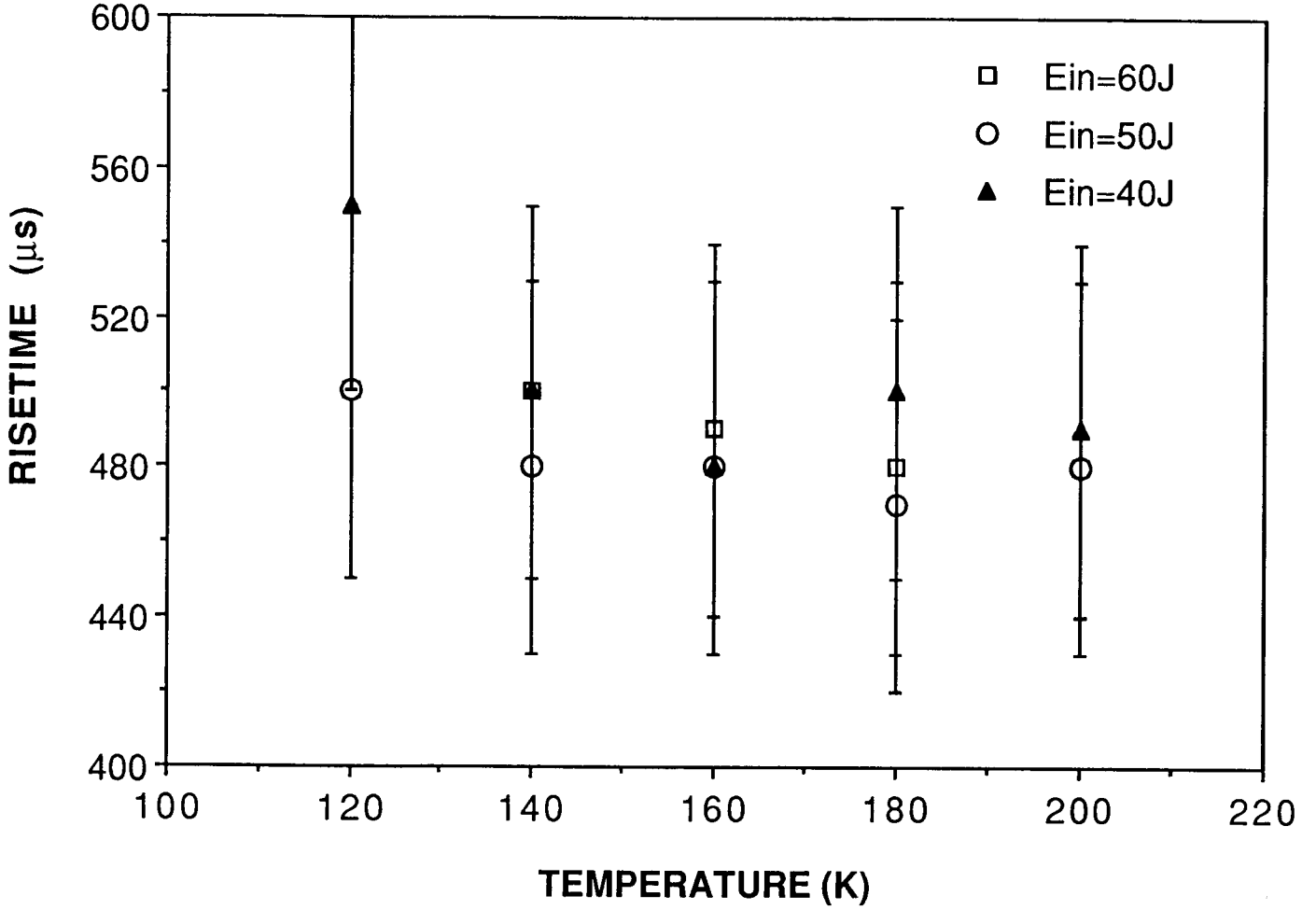

Fig.11 1.9 μm fluorescence risetime of a 0.45Ho:2.5Tm:1.5Cr:YAG crystal as a function of operating temperature at various input energies.

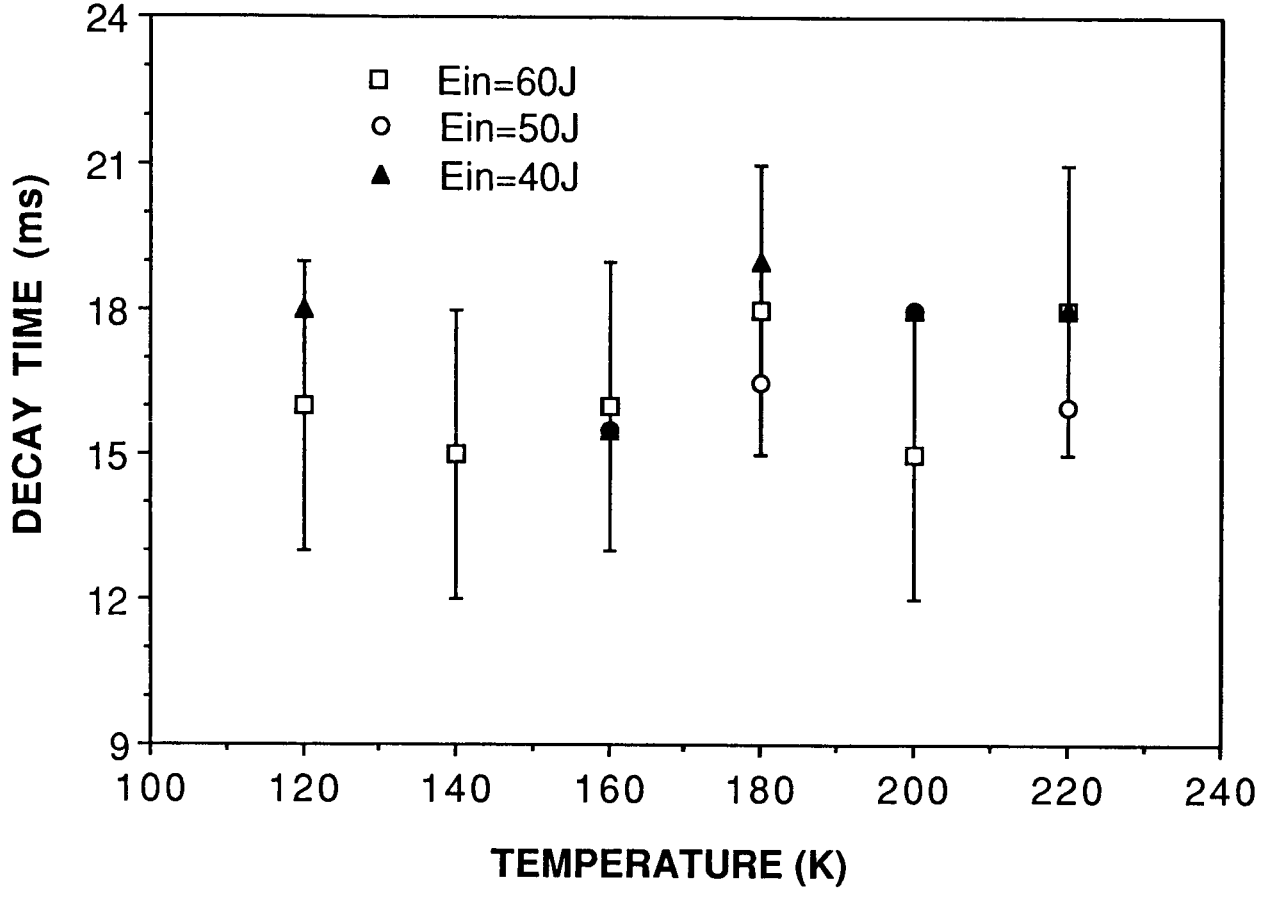

Fig.12 1.9 μm fluorescence decay time of a 0.45Ho:2.5Tm:1.5Cr:YAG crystal as a function of operating temperature at various input energies. (Decay time was taken from 10 % and 90 % of the peak intensity.)

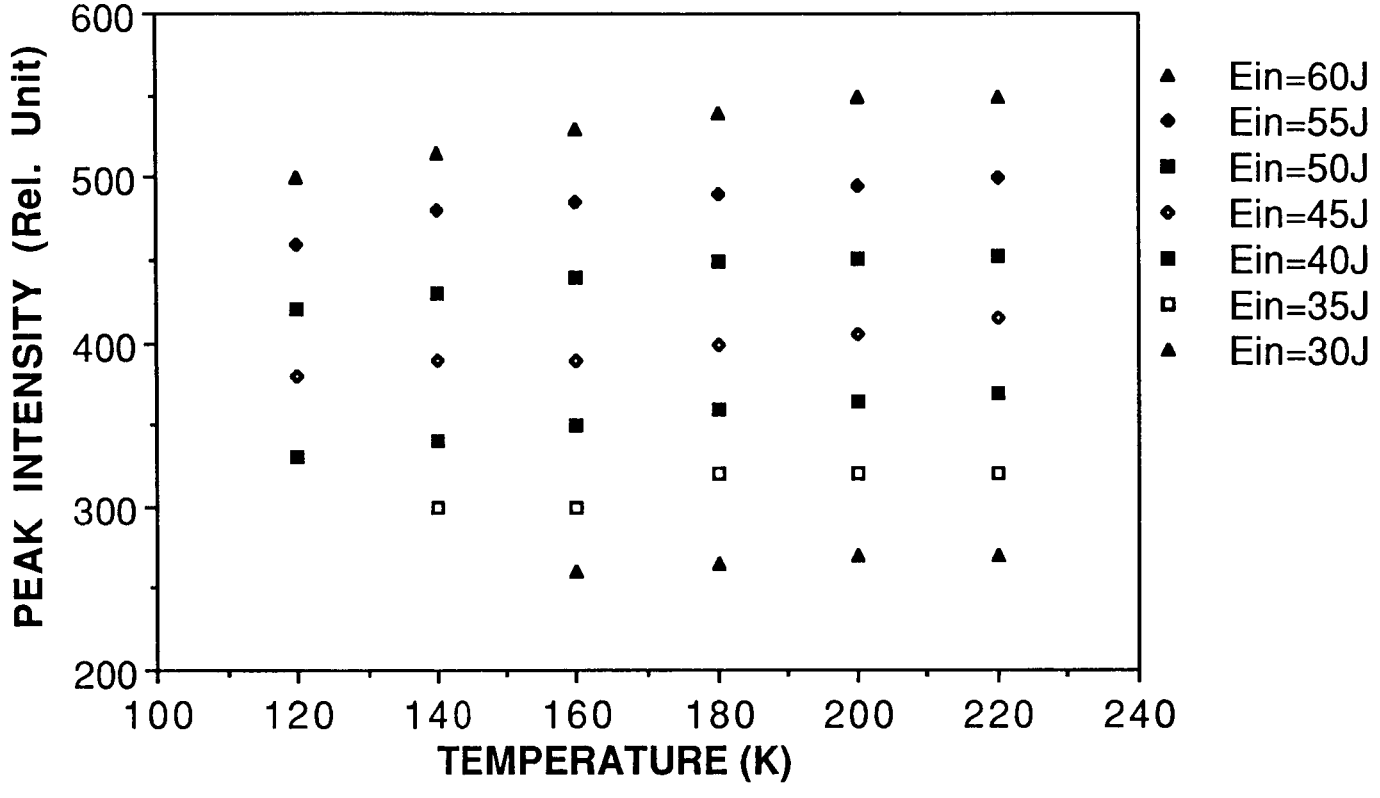

Fig. 13. 1.9 μm fluorescence peak intensity of a 0.45Ho:2.5Tm:1.5Cr: YAG crystal as a function of temperature at various input energies.

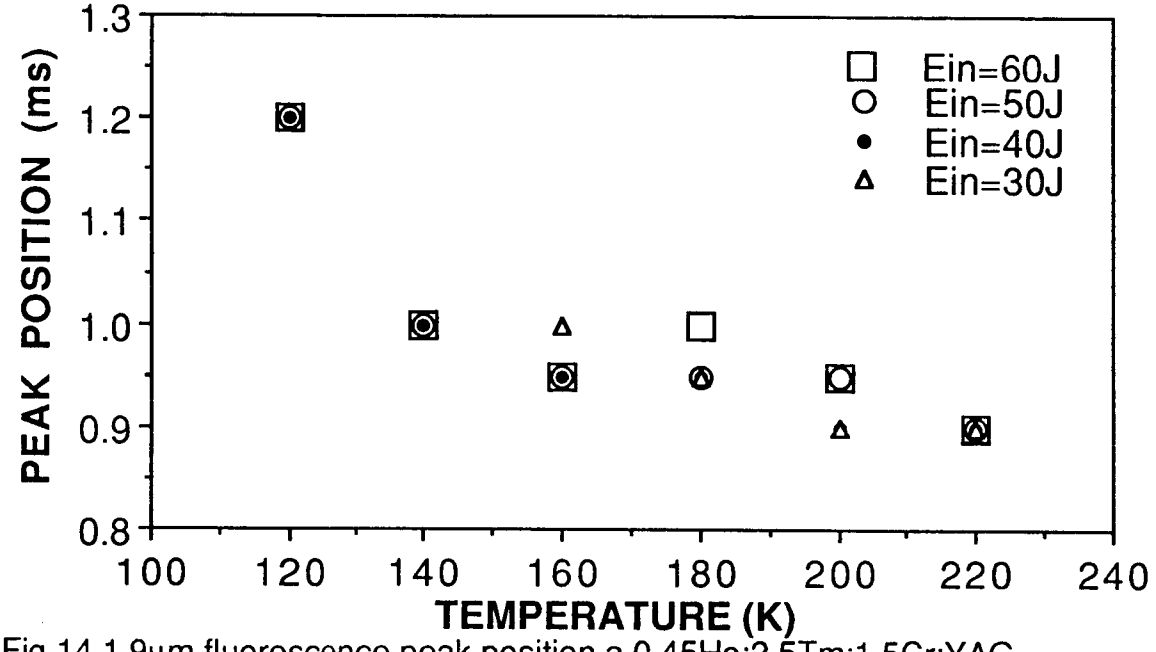

Fig.14 1.9µm fluorescence peak position a 0.45Ho:2.5Tm:1.5Cr:YAG crystal with respect to the beginning of the fluorescence pulses as a function of temperature at various input energies.

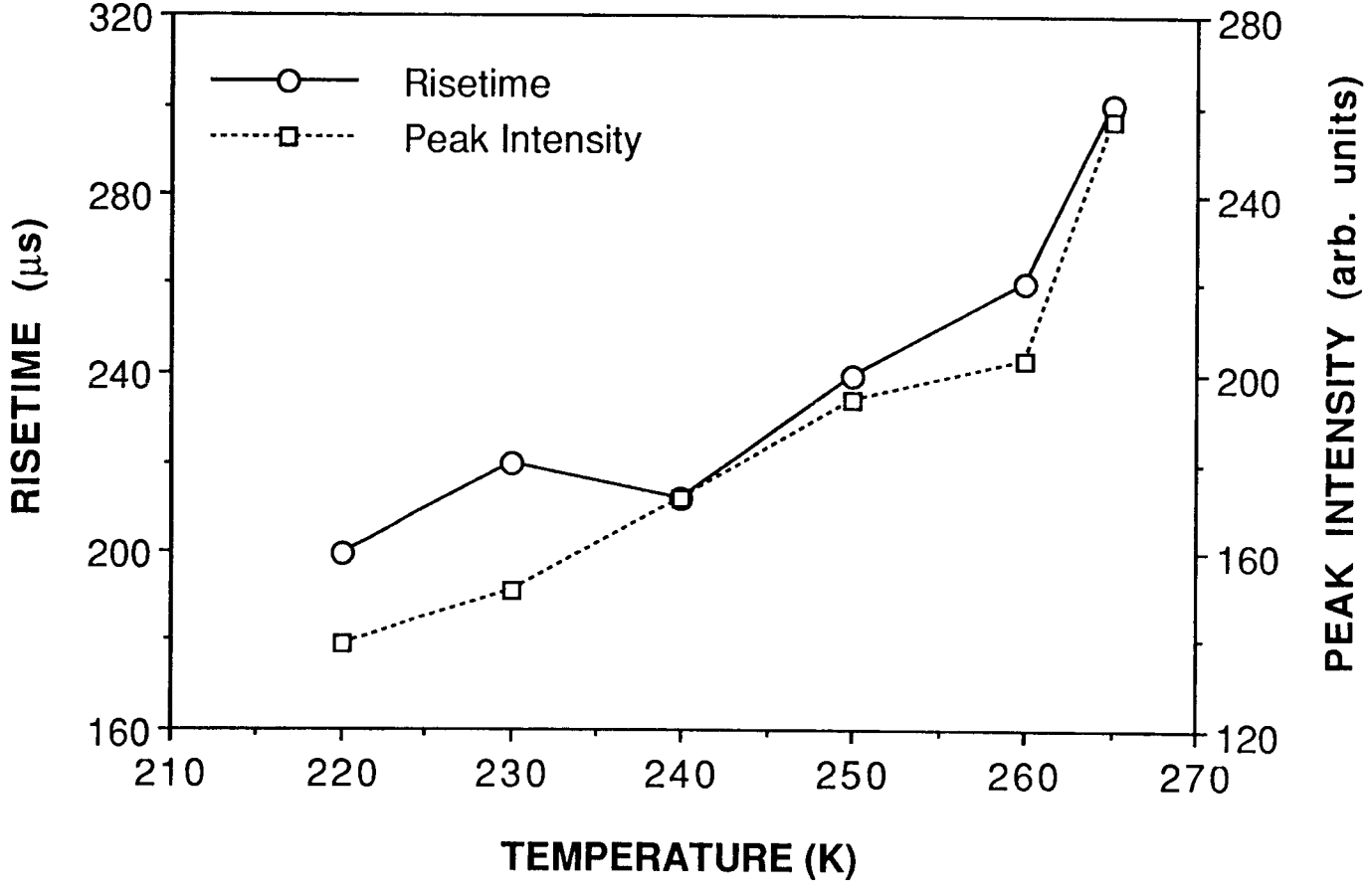

Fig.15 1.7 μm fluorescence risetime and peak intensity of a 0.45Ho:2.5Tm:1.5Cr:YAG crystal as a function of temperature. (Input electrical energy = 60 J)

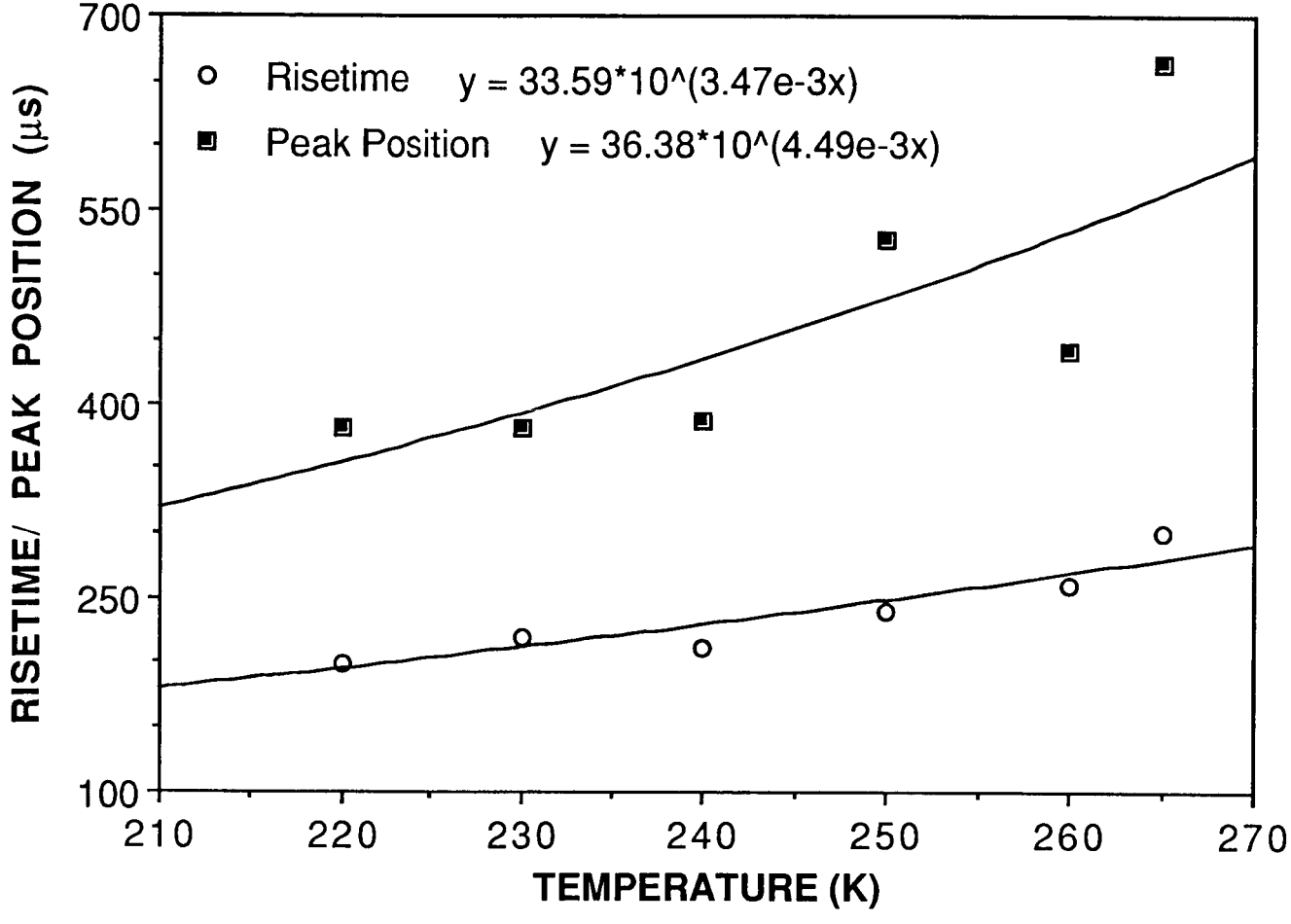

Fig.16 1.7 µm fluorescence peak position and risetime of a 0.45Ho:2.5Tm:1.5Cr:YAG crystal as a function of temperature at input electrical energyof 60 J.

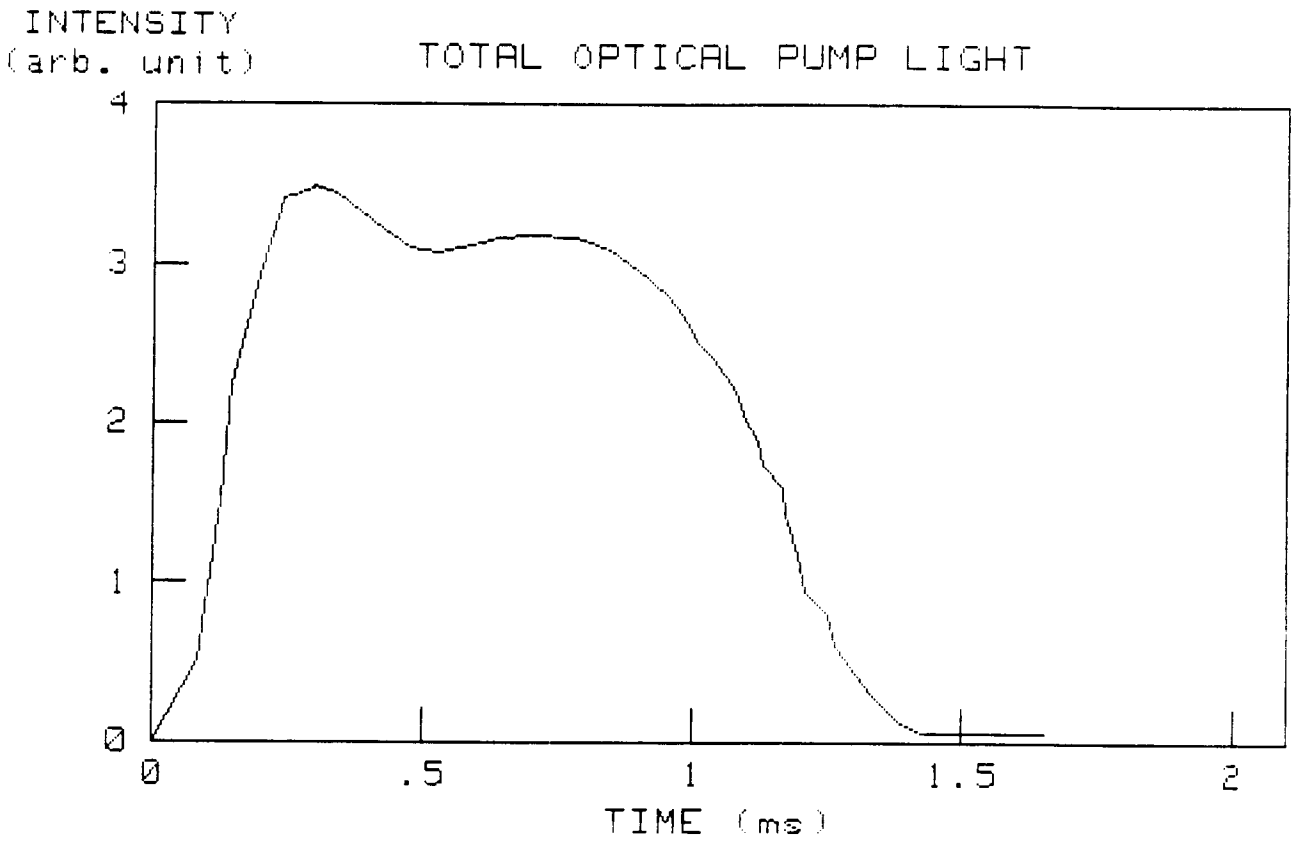

Fig. 17. Total optical flashlamp light measured with a silicon photodiode. A 300 J input energy was used in a 3 LC section PFN designed to have critically damping for that energy and 1 ms pulse width with sectional capacitance and inductance of 150 μF and 185 μH, respectively.

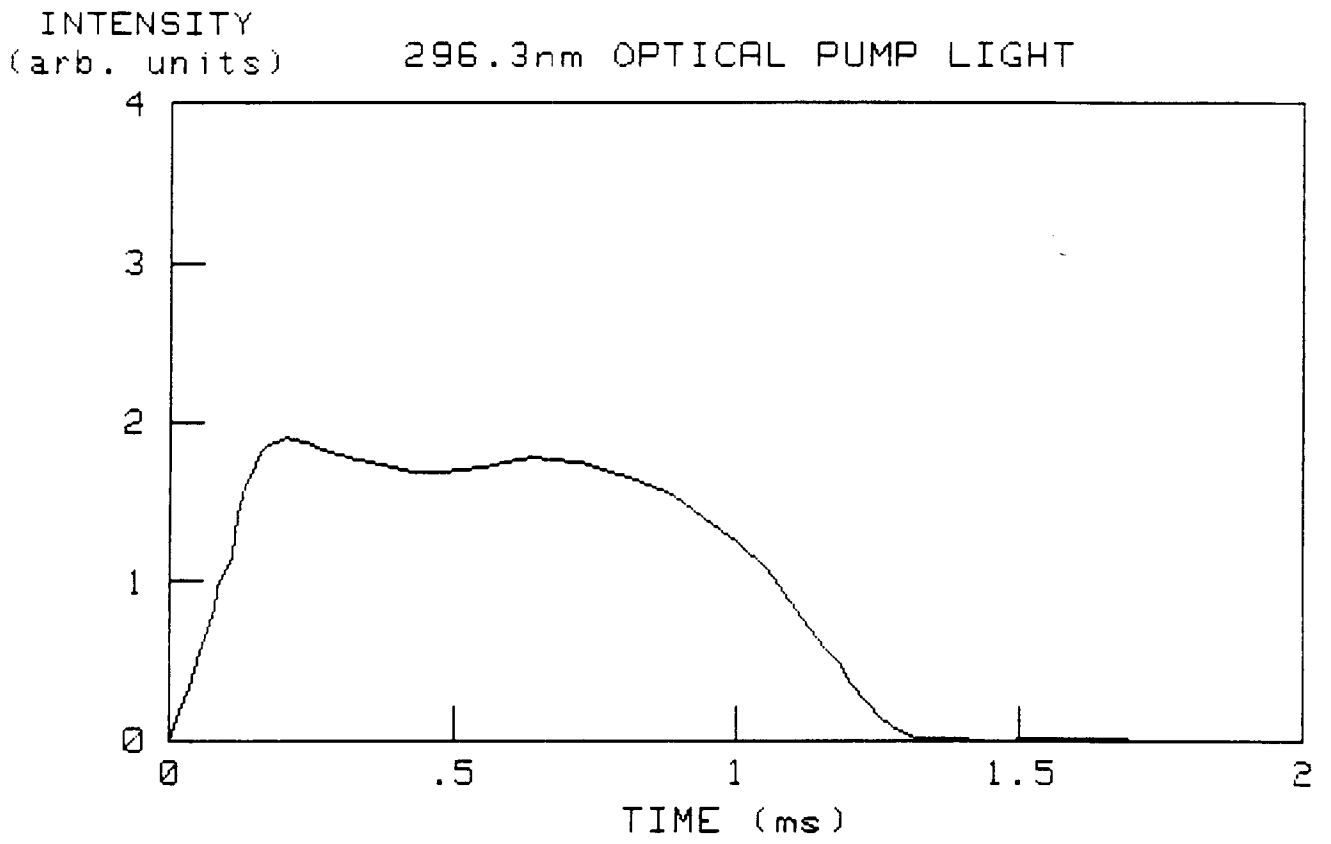

Fig. 18. Flashlamp light signal taken with a 296.3 nm narrow band filter at an input energy of 300 J.

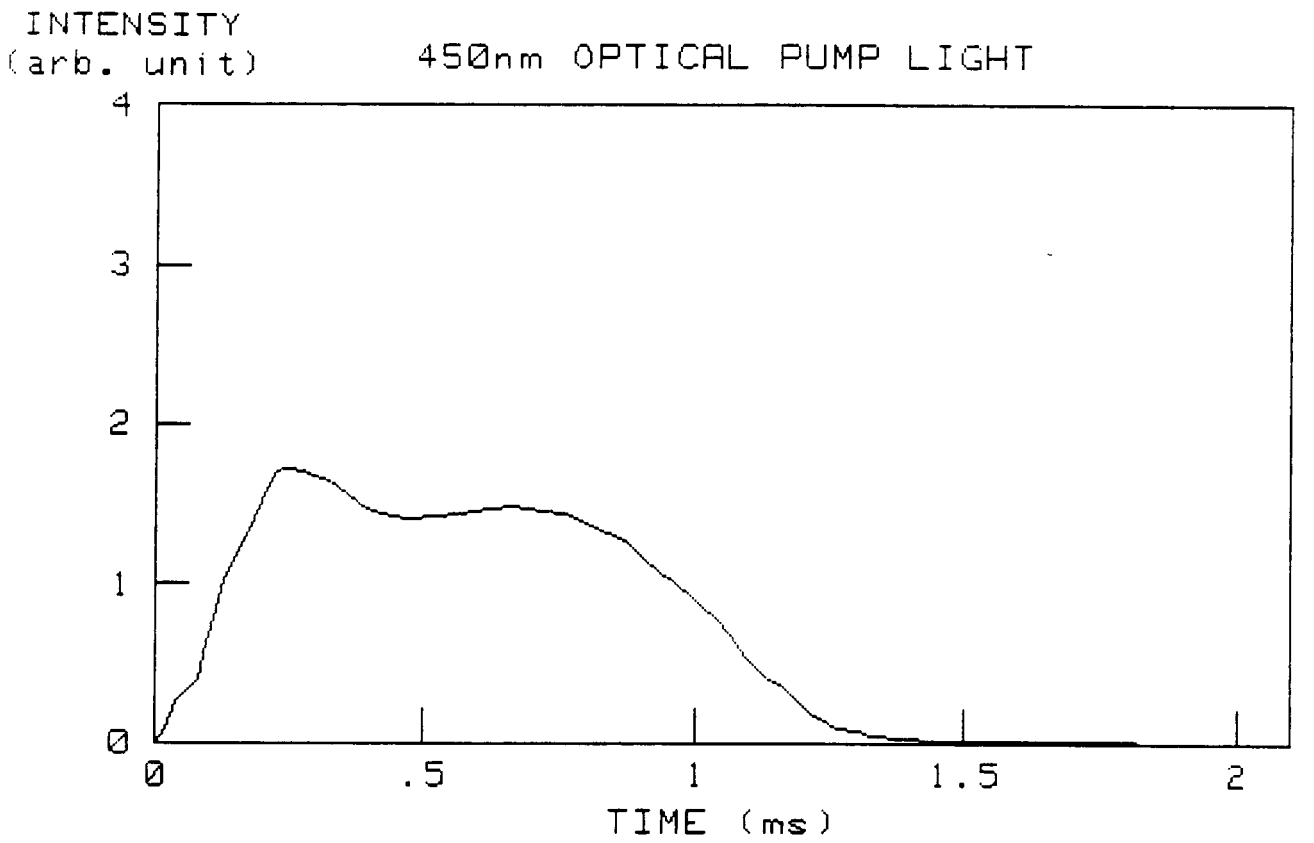

Fig. 19. Flashlamp light signal taken with a 450 nm narrow band filter at an input energy of 300 J.

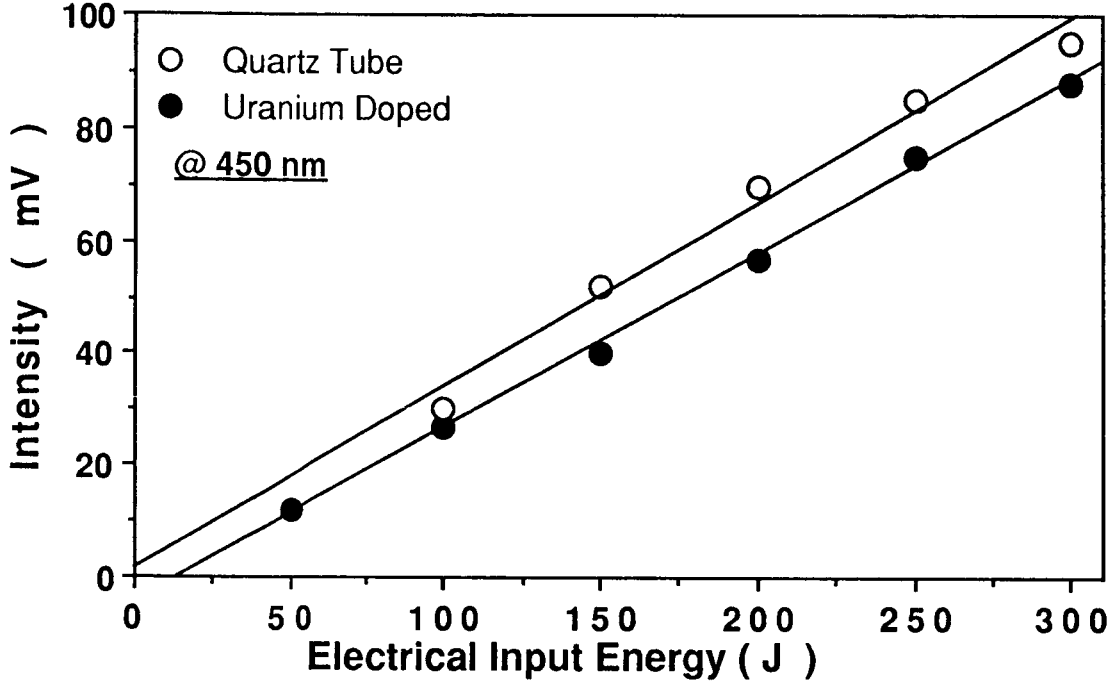

Fig.20 Flashlamp light at 450 nm as a function of electrical input energy.

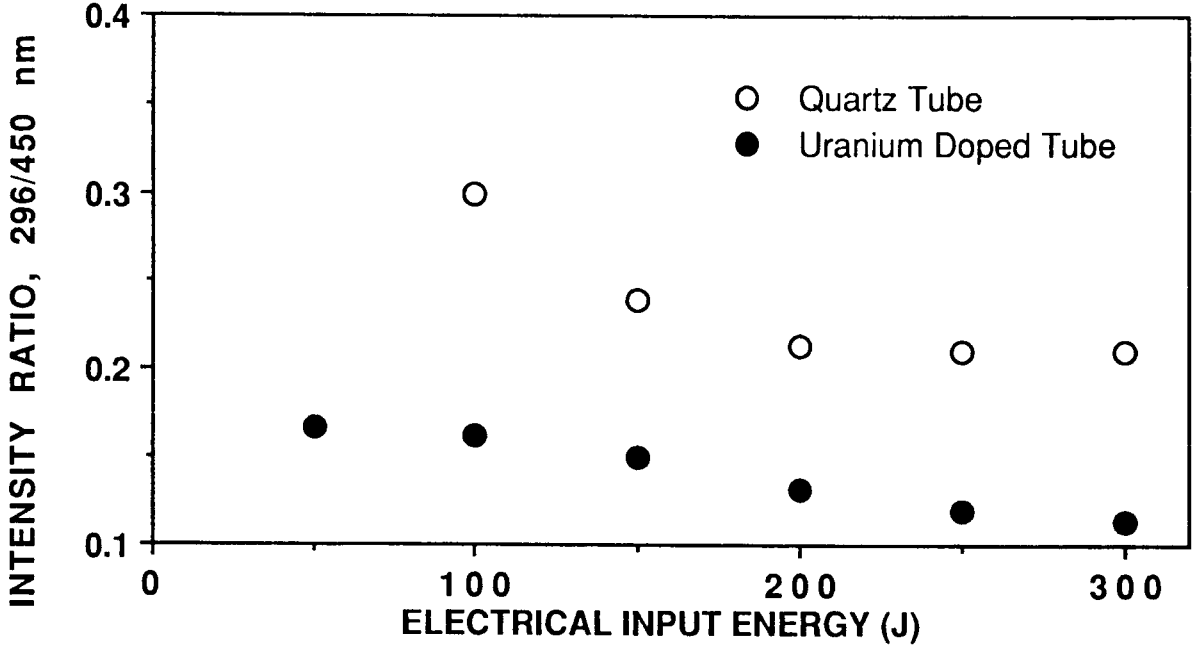

Fig. 21 Ratio of flashlamp light intensity at 296 nm to that at 450 nm as a function of electrical input energy to compare a uranium doped flow tube to a quartz flow tube for UV cut-off effect.

Appendix

(Paper Presented at NASA-HBCU Forum, March 22-23, 1989)

Development of Flashlamp-Pumped Q-switched Ho:Tm:Cr:YAG Lasers for Mid-Infrared Lidar Application

Young S. Choi,[a] Kyong H. Kim,[a] Donald A. Whitney,[a] Robert V. Hess,[b] Norman P. Barnes,[b] Clayton H. Bair,[b] and Philip Brockman[b]

[a]Department of Physics, Hampton University, Hampton, Virginia 23668

and

[b]NASA Langley Research Center, Hampton, Virginia 23665

ABSTRACT

A flashlamp pumped 2.1 μm Ho:Tm:Cr:YAG laser has been studied for both normal mode and Q-switched operations under various operating conditions. Laser output energy, slope efficiency, thresholds and pulse shape were determined as a function of operating temperature, output mirror reflectivity, input electrical energy and Q-switch opening time. The measured normal-mode laser thresholds of a Ho^{3+}(0.45 atomic %):Tm^{3+}(2.5 at. %):Cr^{3+}(0.8 at. %):YAG crystal ranged from 26 to 50 J between 120 to 200 Kelvin degree with slope efficiencies up to 0.36 % with a 60 % transmission. From the Q-switched operations the slope efficiency corresponding to 90 % of the normal-mode operation was also observed.

INTRODUCTION

Development of solid state lasers with Ho^{3+}, Tm^{3+} and(or) Er^{3+}-ion doped crystals have been pursued by NASA for eye-safe and mid-infrared LIDAR (light detection and ranging) application. As a part of the project we have been working on evaluation of $Ho^{3+}:Tm^{3+}:Cr^{3+}$:YAG crystals for normal-mode and Q-switched 2.1 μm laser operations under flashlamp pumping in order to determine an optimum Tm^{3+}-ion concentration in the crystal.

Lasing properties of the Ho^{3+} ion in the mid-infrared region have been studied by many research groups since early 1960's.[1-5] However, the technology of those lasers is still premature for the lidar application. In order to overcome the inefficiency related to narrow absorption bands of the Ho^{3+}, Tm^{3+} and Er^{3+}-ions, the improvement of flashlamp-pumped Ho^{3+} laser efficiency has been demonstrated recently by several research groups[6,7] by utilizing the broad absorption spectrum of Cr^{3+}-ions over the flashlamp's emission spectrum and efficient energy transfer to the Tm^{3+} and then to Ho^{3+}-ions. In the Tm^{3+} and Ho^{3+} combination it is known that high Tm^{3+}concentration and low Ho^{3+} concentration are preferred to achieve a quantum efficiency of 2 and to avoid large reabsorption losses.[6] However, in the Ho^{3+}, Tm^{3+} and Cr^{3+} combination, determination of the optimum Tm^{3+} concentration in the Ho:Tm:Cr:YAG crystal is required to ensure efficient energy transfer from Cr^{3+} to Tm^{3+} and from Tm^{3+} to Ho^{3+}. This paper will present the result obtained so far with one out of the three Ho:Tm:Cr:YAG crystals with 3 different Tm^{3+} concentrations (2.5, 3.5 and 4.5 at. %) at relatively fixed Cr^{3+} (1.5 at. %) and Ho^{3+} (0.45 at. %) concentrations

QUANTUM PROCESSES in Ho^{3+}, Tm^{3+} and Cr^{3+}-IONS

The energy levels of the Cr^{3+}, Tm^{3+} and Ho^{3+}-ions and the energy transfer mechanisms among those ions in a YAG crystal are illustrated in Fig.1. The use of Cr^{3+} for flashlamp pumping is based on its broad absorption spectrum provided by the transitions from the ground $^4A_2$ state to the upper $^4T_1$ and $^4T_2$ states and the near resonant efficient energy transfer to the $^3H_4$ state of the Tm^{3+}-ions. Fig.2 shows the absorption spectrum of the Ho^{3+}(0.45 atomic %):Tm^{3+}(2.5 at. %):Cr^{3+}(1.5 at. % ?):YAG crystal. The chromium concentration of 1.5 atomic % stated by vendor turns out to be 0.8 atomic % from the absorption measurement. The two broad bands correspond to the chromium absorption and other sharp peaks correspond to the absorption by the holmium and thulium ions. Armagan, et al's work(Ref.8) showed that the energy transfer processes is more effective in crystals with low Cr^{3+} and high Tm^{3+} concentrations.

For high Tm concentrations, the transition from the $^3H_4$ state

to the $^3F_4$ state induces the cross relaxation process which provides two $^3F_4$ Tm ions from a single Tm ion in the $^3H_4$ level. As a result, the quantum efficiency approaches to two and quantum energy is lowered down to the infrared region. Then, the near resonant energy transfer process from the $^3F_4$ Tm state to the $^5I_7$ Ho state provides the enhancement of the pumping mechanisms of the Ho-ions. Lasing processes in the Ho^{3+}-ions can be enhanced by codoping the Cr^{3+} and Tm^{3+}-ions in the laser crystal through a double step energy transfer process Cr->Tm and Tm->Ho and cross relaxation Tm->Tm. In order to operate the 2.1 μm Ho laser at room temperature, the Ho^{3+} concentration must be low. The increase of the Ho^{3+} concentration increases the ground state population of $^5I_8$ of Ho level and causes high resonant reabsorption losses for the $^5I_7$(Ho)-$^5I_8$(Ho) laser transition. However, as the temperature goes down, the upper manifolds of the lower laser level ($^5I_8$) of the Ho^{3+}-ion becomes thermally unpopulated and the efficiency of the laser performance increases. Since the upper state lifetime of the Ho^{3+}-ion is longer than 4 ms even at room temperature and provides an efficient storage time for the Q-switch operation, a high Ho ion concentrations may be effective for a high Q-switched laser output.

EXPERIMENTAL METHODS

The experimental configuration used in this research is shown in Fig.3. The temperature of the laser rod was varied from 120 K to room temperature by circulating liquid nitrogen vapor around the rod and the flashlamp was cooled by circulating deionized water. The flashlamp and laser rod were placed in a pumping cavity of a shape of cylindrical ellipse with major and minor axes of 152.4 mm and 149.1 mm respectively and with a 76.2 mm long aluminum reflector. The detailed cavity design was reported elsewhere.[9] In order to achieve thermal insulation, the entire pumping cavity was placed in an vacuum system. Good thermal isolation was necessary since the cooling capacity of liquid nitrogen vapor was limited. A 450 torr Xe flashlamp with 4 mm bore diameter and 76.2 mm arc length was used and surrounded by a uranium doped flow tube water jacket to reduce possible solarization effect. The size of the Ho:Tm:Cr:YAG laser rod used was 4 mm in diameter and 55 mm in length.

Since the Ho:Tm:Cr:YAG has a long upper laser level lifetime, the pulse forming network (PFN) for the flashlamp was designed for long pulse operations. With a 146.5 μF capacitor and a 184 μH inductor critically damped pulses of 300 μs FWHM pulse length were obtained at the input voltage of 905 volts which corresponds to the electrical input energy of 60 J. The highly reflective mirror at 2.1 μm with a 10 m radius curvature is attached to the one end of the vacuum box as a window, and an antireflection coated quartz

flat was placed on the other side of the vacuum box. Flat mirrors with various reflectivities were used as output couplers. The total resonator length was 88 cm. In Q-switched operations a lithium niobate crystal($LiNbO_3$) of dimensions of 9 mm x 9 mm x 25 mm was used as a Q-switch along with a ZnSe plate polarizer of 2.17 mm thickness. The hold-off voltage for the Q-switch crystal was 1.62 kV and the Q-switch trigger signal was delayed from 0 to several ms with respect to the trigger for the flashlamp.

The laser output energy and pulse shape were measured with a pyroelectic energy meter and with a liquid N_2 cooled HgCdTe detector, respectively.

RESULTS

Fig.4 shows the normal-mode laser output energies of the Ho(0.45 %):Tm(2.5 %):Cr(0.8 %):YAG crystal measured as a function of the electrical energy stored in capacitor with various output mirror reflectivities at the operating temperature of 150 K. As expected, the slope efficiency and threshold energy increase with the decreasing mirror reflectivity. The measured normal-mode laser output energies as a function of operating temperature at various electrical input energies with a 60 % reflectivity mirror is shown in Fig.5. The decrease of the laser output energy with the increasing temperature clearly indicates the effect due to thermal population in the lower laser level. Figs. 6 and 7 show the dependency of the laser threshold and slope efficiency respectively on the operating temperature at various mirror reflectivities. The highest slope efficiency of 0.36 % was obtained with a 60 % mirror at 120 K and the lowest extrapolated threshold electrical input energy of 14.8 J was achieved at 120 K with a 98 % mirror. The low slope efficiency may be attributed to the relatively small crystal diameter compared to the mode diameter of about 2.8 mm and poor optical coupling between the flashlamp and the laser rod due to their different length and low cavity reflectivity which was less than 80 % at 633 nm.

The measured Q-switched and normal-mode laser outputs are plotted in Fig.8 as a function of the electrical input energy stored in capacitor at various temperatures. The output mirror used in this comparative measurement had a 60 % reflectivity and the normal-mode operation was done with the Q-switch crystal and ZnSe polarizer in the resonator. The Q-switched laser output and slope efficiency are lower and threshold is higher than those of normal mode operation. The observed slope efficiencies are 0.123 % for normal-mode and 0.111 % for Q-switched operation at the operating temperature of 130 K. The Q-switched slope efficiency of the Ho:Tm:Cr:YAG crystal corresponds approximately 90 % of the normal-mode slope efficiency. The measured wavelength of the Ho:Tm:Cr:YAG laser with a spectrometer was about 2.095 μm.

CONCLUSION

A Ho:Tm:Cr:YAG laser with ion concentrations of 0.45 at. % Ho, 2.5 at. % Tm and 0.8 at. % Cr has been studied for both normal mode and Q-switched 2.1 μm laser operation under flashlamp pumping at various operating temperatures, various output mirror reflectivities, and various input energies. Continuous work on the evaluation of the other two crystals with different Tm^{3+}-ion concentrations is under progress and will provide an optimum Tm concentration in the Ho:Tm:Cr:YAG crystal.

ACKNOWLEDGEMENT

This work was supported by NASA under grant number NAG-1-877. We acknowledge that Mark E.Storm and Coherent Technology provided the laser crystals and Lewis G. Burney, Donald Gettemy, Edward A. Modlin, and Keith E. Murray provided the technical support during the course of this research work. We also appreciate valuable discussion with Dr. Alfred M. Buoncristiani.

REFERENCES

1. L. F. Johnson, G. D. Boyd, K. Nassau, Proc. IRE, **1962**, 50, 87
2. E.P. Chicklis, C. S. Naiman, R. C. Folweileer, D. R. Gabbe, H. P. Jenssen, and A. Linz, Appl. Phys. Lett. **1971**, 19(4), 119.
3. N. P. Barnes and D. J. Gettemy, IEEE J. Quantum Electron., **1981**, QE-17(7), 1303.
4. H. Lotem, Y. Kalisky, J. Kagan, and D. Sagie, IEEE J. Quantum Electron., **1988**, 24(6), 119.
5. E. W. Duczynski and G. Huber, Appl. Phys. Lett., **1986**, 48(23), 1562.
6. P. Mitzscherlich, Tunable Solid-State Lasers II (Edited by Budgor, *et al.*), Springer-Verlag, New York, **1986**, p. 282.
7. I. A. Shcherbakov, Tunable Solid-State Lasers II (Edited by Budgor, *et al.*), Springer-Verlag, New York, **1986**, p. 293.
8. G. Armagan, B.Di Bartolo and A. M. Buoncristiani, "Spectroscopic Investigation of the Cr to Tm Energy Tansfer in Yttrium Aluminum Garnet Crystals," to be published. (**1989**).
9. D. Gettemy, N. P. Barnes, and E. Griggs, **51**(9), 1194 (1980).

ORIGINAL PAGE IS
OF POOR QUALITY

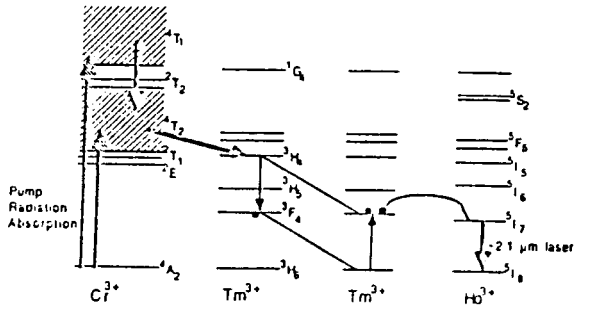

Fig.1 Energy transfer processes in a Ho:Tm:Cr:YAG crystal.

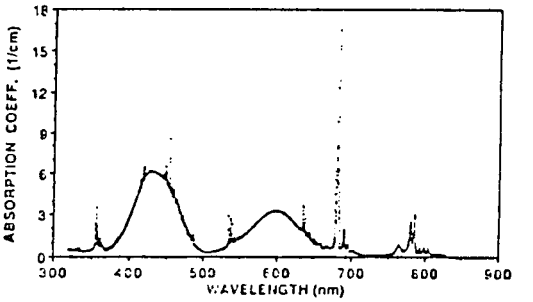

Fig.2 Absorption spectrum of the Ho:Tm:Cr:YAG crystal (0.45% Ho, 2.5% Tm, 0.8% Cr).

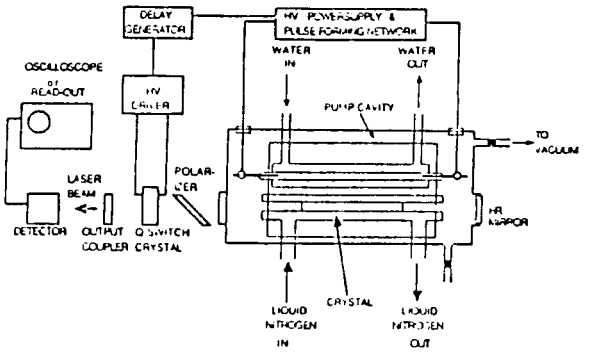

Fig.3 Schematic diagram for the experimental setup.

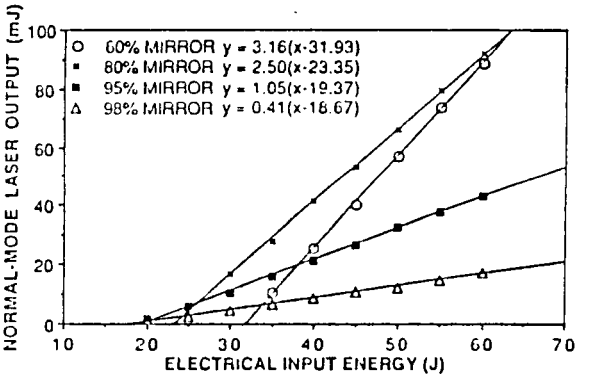

Fig.4 Normal-mode laser output energy of the Ho:Tm:Cr:YAG crystal as a function of electrical input energy at 150 K.

ORIGINAL PAGE IS
OF POOR QUALITY

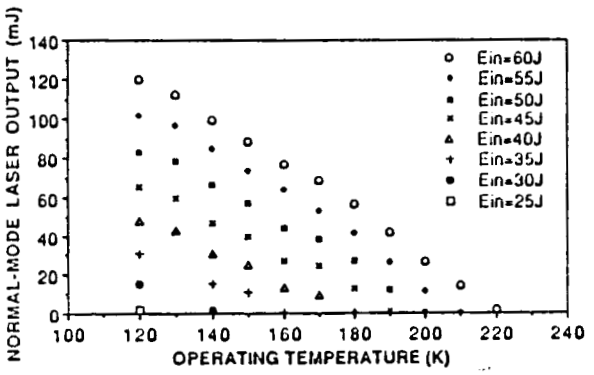

Fig.5 Normal-mode laser output energy as a function of the operating temperature with a 60 % reflectivity output mirror.

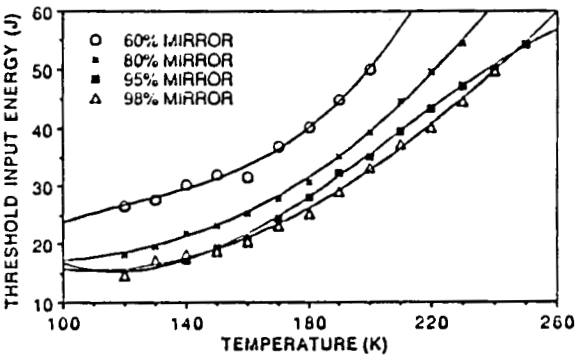

Fig.6 Threshold input electrical energy as a function of the operating temperature with various output mirror reflectivities.

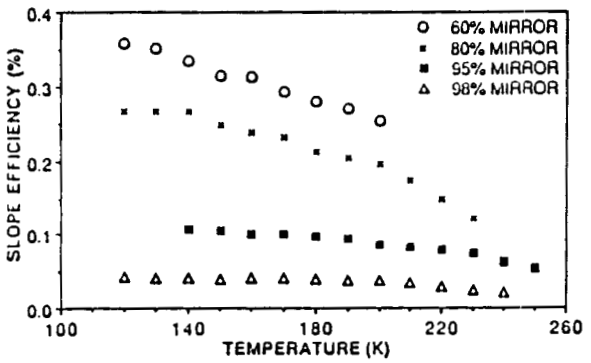

Fig.7 Slope efficiency as a function of temperature with various mirror reflectivities.

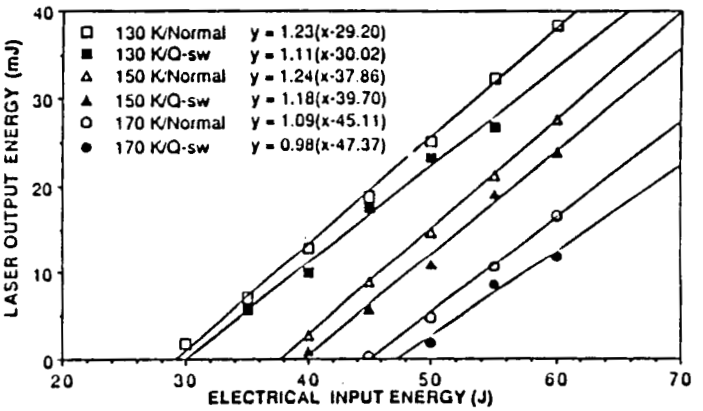

Fig.8 Normal-mode and Q-switched laser output energies as a function of the input energy with a 60 % reflective mirror.